Fast erg K^+ currents in rat embryonic serotonergic neurones

Wiebke Hirdes[1], Michaela Schweizer[2], Kristina S. Schuricht[1], Saskia S. Guddat[1], Iris Wulfsen[1], Christiane K. Bauer[1] and Jürgen R. Schwarz[1]

[1] *Institute of Applied Physiology, University Hospital Hamburg-Eppendorf, University of Hamburg, Martinistr. 52, D-20246 Hamburg, Germany*
[2] *Center for Molecular Neurobiology, ZMNH, University of Hamburg, Falkenried 94, D-20251 Hamburg, Germany*

***Ether-à-go-go*-related gene (erg) channels form one subfamily of the *ether-à-go-go* (EAG) K^+ channels and all three erg channels (erg1–3) are expressed in the brain. In the present study we characterize a fast erg current in neurones in primary culture derived from the median part of rat embryonic rhombencephala (E15–16). The relatively uniform erg current was regularly found in large multipolar serotonergic neurones, and occurred also in other less well characterized neurones. The erg current was blocked by the antiarrhythmic substance E-4031. Single-cell RT-PCR revealed the expression of erg1a, erg1b, erg2 and erg3 mRNA in different combinations in large multipolar neurones. These cells also contained neuronal tryptophan hydroxylase, a key enzyme for serotonin production. To characterize the molecular properties of the channels mediating the native erg current, we compared the voltage and time dependence of activation and deactivation of the neuronal erg current to erg1a, erg1b, erg2 and erg3 currents heterologously expressed in CHO cells. The biophysical properties of the neuronal erg current were well within the range displayed by the different heterologously expressed erg currents. Activation and deactivation kinetics of the neuronal erg current were fast and resembled those of erg3 currents. Our data suggest that the erg channels in rat embryonic rhombencephalon neurones are heteromultimers formed by different erg channel subunits.**

(Resubmitted 24 December 2004; accepted 26 January 2005; first published online 27 January 2005)
Corresponding author J. R. Schwarz: Institute of Applied Physiology, University Hospital Hamburg-Eppendorf, Martinistr. 52, D-20246 Hamburg, Germany. Email: schwarz@uke.uni-hamburg.de

Ether-à-go-go-related gene (erg) K^+ currents are among the near-threshold ion currents modulating excitability. The three erg channels which have been cloned (erg1: Warmke & Ganetzky, 1994; erg2, erg3: Shi *et al.* 1997) form a subfamily of the *ether-à-go-go* (EAG) voltage-gated K^+ channels (reviewed by Bauer & Schwarz, 2001). Splice variants of erg1 with shorter N-terminals have also been found, erg1a′ (London *et al.* 1997) and erg1b (London *et al.* 1997; Lees-Miller *et al.* 1997). The cardiac rapidly activating K^+ current (I_{Kr}) is conducted by channels formed by erg1 subunits (Sanguinetti *et al.* 1995). The ion channels mediating I_{Kr} have been shown to inactivate faster than they activate (Shibasaki, 1987). Because all erg channels share this peculiar gating behaviour, these channels are functionally inward rectifiers.

Erg channels have been thoroughly analysed in cardiac myocytes, neuroblastoma cells and lactotropes. I_{Kr} contributes to repolarizing the heart action potential, and abnormal function of erg1 channels may prolong it, leading to arrhythmia and eventually sudden death (LQT2 syndrome; Sanguinetti *et al.* 1995; Curran *et al.* 1995). In neuroblastoma cells, erg currents have been shown to be involved in frequency adaptation (Chiesa *et al.* 1997), neuritogenesis (Arcangeli *et al.* 1993) and regulation of the cell cycle (Arcangeli *et al.* 1995). In lactotropes, the erg-mediated current contributes to the maintenance of the resting potential (Bauer *et al.* 1990; Barros *et al.* 1992) and erg current reduction by thyrotropin-releasing hormone increases prolactin secretion (Bauer *et al.* 1999). Erg currents have also been described in gastro-intestinal and vascular smooth muscle cells (Ohya *et al.* 2002*a*,*b*), pancreatic β-cells, cells of the carotid body and various tumour cell lines (reviewed by Bauer & Schwarz, 2001).

In rat brain the transcripts of the three erg channels have been shown to be differentially expressed (Saganich *et al.* 2001). Strong expression was found for erg1, erg2 and erg3 in the olfactory bulb, for erg1 in brainstem nuclei including the raphe nuclei and in the cerebellum, and for erg3 in the cerebral cortex and hippocampal pyramidal cells. A recent study by Papa *et al.* (2003) confirmed these results, but also

 DOI: 10.1113/jphysiol.2004.082123

demonstrated a more generalized expression of the three erg channel subunits in the rat brain. In embryonic mouse brain (E9.5) all three erg mRNAs are present throughout the brain changing to a more differentiated expression at E13.5 (Polvani *et al.* 2003). Erg1 channels have also been found in rat hippocampal astrocytes where they have been assumed to contribute to K^+ homeostasis (Emmi *et al.* 2000).

So far, the only description of a neuronal erg current has been in mice Purkinje cells (Sacco *et al.* 2003). In the present study we show that an erg current can also be recorded from rhombencephalic neurones in primary culture of embryonic rats (E15/16). This neuronal erg current activates and deactivates faster than HERG current (Wang *et al.* 1997) and the erg current in lactotropes (Bauer *et al.* 1990; Schäfer *et al.* 1999). Using single-cell RT-PCR we demonstrate that different combinations of erg subunits or splice variants are expressed in these neurones. This finding, together with the comparison of some biophysical properties of the neuronal erg current with those of heterologously expressed erg1a, erg1b, erg2 and erg3 currents, suggests that the rhombencephalic erg current is mediated by heteromeric channels. Part of the results have been published in abstract form (Schwarz *et al.* 2003).

Methods

Primary culture

Timed pregnant rats at 15 or 16 days in gestation, the day following nocturnal mating being considered as E1, were killed by decapitation under halothane anaesthesia (Willy Rüsch GmbH, Kernen, Germany) and the embryos were removed. The rhombencephalon containing the raphe nuclei was microdissected at the rhombencephalic isthmus and cervical flexure (König *et al.* 1987). The middle parts containing the serotonin-immunopositive cells were further separated and incubated in an enzyme solution (0.5 units papain (Worthington Biochemical Corporation, NJ, USA) per millilitre Earle's balanced salt solution (Gibco-Invitrogen, Karlsruhe, Germany) containing 0.1 mM EDTA and 0.2 mM cysteine) for 20 min at 37°C. The cells were gently triturated and the dissociated cells were plated on 12 mm diameter round glass cover slips coated with poly-L-lysine and laminin (Sigma, Taufkirchen, Germany), placed in 24-well plates with plating medium (minimal essential medium (MEM, Gibco-Invitrogen) enriched with 10% horse serum (Gibco-Invitrogen) and 6% glucose). Three hours after plating, two-thirds of the plating medium was exchanged for normal growth medium (MEM enriched with 0.1% ovalbumin, 5 μg ml^{-1} insulin, 1 mM pyruvate, 0.1 mM putrescine, 0.02 μM progesterone, 0.03 μM selenium, 100 μg ml^{-1} transferrin and 6% glucose (Sigma)). Cells were used for up to 9 days. Animal care and experimental procedures were in accordance with the guidelines laid down by the animal welfare committee of the University Hospital Hamburg-Eppendorf.

Molecular biology

Cloning of r-erg1b. The alternatively spliced part was amplified from rat pituitary cDNA by PCR. Primers were constructed against the rat genomic sequence part reflecting the specific mouse erg1b exon (5′-ATGGC-GATTCCAGCCGGGAA-3′) and a shared exon of the r-erg1 sequence (Z96106) (5′-CTCCTCAGAGC-CAGAGCCAA-3′). The amplified cDNA fragment was cloned into the r-erg1 cDNA sequence at the *Hpa*I site.

Heterologous expression in CHO cells. CHO cells were cultured in a medium containing MEM (Gibco-Invitrogen), supplemented with 10% fetal calf serum (PAA, Cölbe, Germany) and 100 U ml^{-1} penicillin, 0.1 mg ml^{-1} streptomycin and 0.3 mg ml^{-1} L-glutamine (Gibco-Invitrogen). Cells were plated on poly-D-lysine (Sigma)-coated CELLocate glass plates (Eppendorf, Hamburg, Germany). The plates were kept in 35 mm plastic culture dishes (Nunc, Rochester, USA). Cells were injected with cDNA one day after passaging and patch-clamped the following day. The cells were injected with an Eppendorf Transjector 5246 (Eppendorf) with cDNA encoding r-erg1a (erg1a; Bauer *et al.* 1998), r-erg1b (erg1b), r-erg2 (erg2) or r-erg3 (erg3; erg2 and erg3 were kindly provided by Dr J. Dixon, State University of New York, Stony Brook, NY, USA) together with EGFP-N1 (Clontech, Heidelberg, Germany). All constructs were cloned into the pcDNA3 vector (Invitrogen, Karlsruhe, Germany).

Reverse transcription PCR. RT-PCR was performed as described by Monyer & Jonas (1995). For single-cell RT-PCR patch pipettes were filled with intracellular solution without ATP and GTP. After the whole-cell configuration was established, the cell content of the neurone was harvested into the patch pipette by applying negative pressure by suction. Using positive pressure the content of the patch pipette was expelled into a PCR tube. The total volume was filled up to 7 μl with intracellular solution. Reverse transcription was carried out in a volume of 10 μl adding following substances to the indicated final concentrations: 2 mM Tris/HCl (pH 8.0), 10 mM DTT, 0.5 mM of each dNTP, 5 μM pd(N6) random hexamer 5′-phosphate (Amersham Pharmacia Biotech, Freiburg, Germany), 20 U RNAguard (Amersham), 100 U M-MLV reverse transcriptase (Invitrogen). The whole volume was subsequently used in a multiplex PCR. The cDNA was amplified with 1.25 U of Taq DNA polymerase (Stratagene, Amsterdam, the Netherlands) in buffer containing 50 mM KCl, 10 mM Tris-HCl (pH 8.8), 0.001% gelatin, 1.5 mM $MgCl_2$ and 0.2 mM of

each dNTP (Invitrogen) in 50 μl reaction assays using 5 pmol of forward and reverse oligonucleotide primers specific for the *r-erg* cDNAs. For the amplification we used the following forward and reverse primer pairs with the GenBank database accession numbers in brackets. *R-erg1* (Z96106): first amplification (nucleotides 2563–3290): 5′-TGGTCTAGCCTGGAGATCA-3′ and 5′-GGGGACGTGGAAGTGG-3′; second amplification (nucl. 2602–3175): 5′-AACATGATTCCTGGCTCCC-3′ and 5′-GGGTTTCCAGCCTGTTCAG-3′. *R-erg1a* (Z96106): first amplification (nucl. 1–353): 5′-ATGC-CGGTGCGGAGGGGCCA-3′ and 5′-TCATTCTTCACG-GGCACCAC-3′; second amplification (nucl. 23–330): 5-TCGCGCCGCAGAACACCTTC-3′ and 5-CACCAAA-CACAGGAAGCAGC-3′. *R-erg1b* (AY669863): first amplification (nucl. 1–754): 5′-ATGGCGATTCCAGCC-GGGAA-3′ and 5′-GGTCGCCCAAGTTGTGCAGC-3′; second amplification (22–754): 5′-GAGAGCAGGAC-AGGGGCTCT-3′ and 5′-GGTCGCCCAAGTTGTG-CAGC-3′. *R-erg2* (AF016192): first amplification (nucl. 2192–2851): 5′-TCTCCAGTCAACACCCCGAC-3′ and 5′-CTCTGGAACTCTAGCTGCTT-3′; second amplification (nucl. 2238–2649): 5′-GGCTTCTTCCTCAATGACAG-3′ and 5′-TCCTGGGTGTCTGAATATGG-3′. *R-erg3* (AF 016191): first amplification (nucl. 2815–3428): 5′-CTGAAGGGGACACCTGTAAG-3′ and 5′-GGGCCTC-TGGTACTCTGCTC-3′; second amplification (nucl. 2826–3418): 5′-ACCTGTAAGCTTCGAAGAAG-3′ and 5′-TACTCTGCTCCTGCGGTCAC-3′. Neuronal tryptophan hydroxylase, *TPH2* (NM_173839): first amplification (nucl. 161–810): 5′-GGAGAGGGTTGT-CCTTGGAT-3′ and 5′-GCAAGCATGAGTGGGGTAGA-3′; second amplification (nucl. 181–740): 5′-TCAGC-GGTGCCAGAAGAGCA-3′ and 5′-GTGTATTCCACCC-TGGGAAT-3′. Glial fibrillary acidic protein, *GFAP* (NM_017009): first amplification (nucl. 516–1120): 5′-AGAACAACCTGGCTGTGTAC-3′ and 5′-CCTGTAGG-TGGCGATCTCGA-3′; second amplification (nucl. 551–1097): 5′-GAAGCCACCTTGGCTCGTGT-3′ and 5′-CCAGGGCTAGCTTAACGTTG-3′. For the first multiplex PCR amplification a predenaturation step at 94°C for 1 min was followed by 40 cycles of three 1 min temperature steps (94°C, 49°C and 72°C) terminated by an elongation step at 72°C for 5 min. In the second amplification the same cycle protocol was used with different annealing temperatures for the individual nested primer pairs, calculated from their G/C and A/T content. Amplified DNA fragments were analysed by agarose gel electrophoresis and sequenced. Negative controls using H_2O, extracellular solution and reverse transcription products generated without enzyme instead of cDNA as template were included. Expected lengths of the amplicons were: erg1 (540 bp), erg1a (330 bp), erg1b (730 bp), erg2 (411 bp), erg3 (568 bp), TPH2 (560 bp) and GFAP (547 bp).

Immunochemistry

Immunohistochemistry. Antibodies against erg1 (Chemicon, Hofheim, Germany, 1 : 500; Pond *et al.* 2000), serotonin (Chemicon, 1 : 100), and TPH (Sigma, 1 : 500) were applied on embryonic rat E15 rhombencephalon whole mounts. Negative controls were performed after preabsorption with the antigen. Neurobiotin-filled neurones were identified with Cy3-conjugated avidin (Camon, Wiesbaden, Germany). These previously whole-cell patch-clamped identified neurones were not clearly serotonin immunopositive, possibly due to loss of the antigen, although many neighbouring neurones were stained. The same observation had been made by Bayliss *et al.* (1997). Therefore we used the TPH antibody to identify serotonergic neurones. Tissue or cell cultures were washed in phosphate-buffered saline (PBS), fixed in 4% paraformaldehyde or formaldehyde, respectively, and washed with PBS. Alexa Fluor 488 or Alexa Fluor 546 (Invitrogen-Molecular Probes, Karlsruhe, Germany, 1 : 1000) was used as secondary antibody. Images were taken on a Leica SP2 confocal microscope with Leica confocal software (Leica Microsystems AG, Heidelberg, Germany).

Western blots. Membrane preparations of primary cell culture, adult rat brain or cell lines were performed as follows. Cells or tissue were washed with cold PBS, collected and homogenized in lysis buffer (25 mM Tris-HCl, 250 mM sucrose, 20 mM EDTA; protease inhibitors: 2 μg ml^{-1} leupeptin, aprotinin and pepstatin A (Sigma), 0.1 mM PMSF (Sigma), 2 mM Na_3O_4V (Merck-Calbiochem), pH 7.2) and incubated on ice for 10 min. After centrifuging for 5 min at 800 *g*, cell debris was removed and the supernatant again centrifuged for 30 min at 48 000 *g*. The pellet containing the cell membranes was resuspended in lysis buffer and stored at −80°C until SDS-PAGE separation and immunoblotting. The erg1 antibody (Chemicon) is targeted against the C-terminus of the human correlate of erg1, HERG1 (aa 1145–1159). According to the manufacturer, it recognizes bands representing erg1a at 175 and 205 kDa (glycosylated) or 135 and 165 kDa (deglycosylated) and a band at 95 kDa representing erg1b, as has been shown by Western blot (Pond *et al.* 2000). Expected molecular weights of unglycosylated erg proteins are: erg1a (127 kDa), erg1a′ (120 kDa), erg1b (90 kDa).

Electrophysiology

Neurones and CHO cells were patch clamped using an EPC-9 amplifier (HEKA Elektronik, Lambrecht, Germany) with Pulse 8.65 software (HEKA). Pipette resistance was < 6 MΩ, series resistance was < 15 MΩ and compensated > 60%. All experiments were performed at room temperature. The liquid junction potential

error (< 3.4 mV) was not corrected. A bath solution with elevated K^+ and low free Ca^{2+} was used that contained (mM): 100 NaCl, 40 KCl, 4 $MgCl_2$, 1 $CaCl_2$, 2.5 EGTA, 10 Hepes, 5 glucose, pH adjusted to 7.3 with NaOH (50 nM free Ca^{2+}; Patcher's Power tools, MPI, Göttingen, Germany). Erg currents were isolated as difference currents with 10 μM of the erg-channel blocker E-4031 (Eisai, Tokyo, Japan) in the bath solution. This relatively high inhibitor concentration was chosen to achieve fast erg current block and minimize rundown artefacts. Erg currents can easily be distinguished from *ether-à-go-go* (eag) currents, which are also blocked at this concentration (Gessner & Heinemann, 2003). There were no indications that other inward currents like inwardly rectifying potassium currents contributed to the difference currents. The pipette solution contained (mM): 140 KCl, 2 $MgCl_2$, 1 $CaCl_2$, 2.5 EGTA, 10 Hepes, 3 Mg-ATP, 0.3 Na_4GTP (44 nM free Ca^{2+}), pH adjusted to 7.3 with KOH, yielding a final K^+ concentration of ~150 mM. For labelling, 0.2% neurobiotin tracer (Vector laboratories Inc. Burlingame, CA, USA) was added. All chemicals were dissolved in water.

Data were analysed with PulseFit 8.65 (HEKA), IgorPro 4.04 (Wavemetrics, Lake Oswego, OR, USA) and Excel (Microsoft, Redmond, WA, USA). All data are presented as means ± S.E.M. Student's two tailed, two-sided *t* test was performed to test for significance. Boltzmann fits were done in Igor and the midpoint voltages are given as $V_{1/2}$ and the slope factors as *k*.

Results

An erg current in embryonic rhombencephalon neurones

In the nervous system of the quail (Crociani *et al.* 2000) and the mouse (Polvani *et al.* 2003) erg channel subunits have been found to be expressed at early embryonic stages. Using an antibody against erg1 subunit protein (Pond *et al.* 2000) we found an intense staining in different nuclei of the embryonic (E15) rat brainstem which was especially strong in raphe neurones (Fig. 1). This finding confirms results of Saganich *et al.* (2001), who demonstrated in adult rat brain a very high expression of erg1 channel subunits at the mRNA level in the brainstem, including the raphe nuclei. Figure 1 shows that the majority of erg1-positive neurones were serotonergic. To investigate whether erg currents can be recorded from raphe neurones, rat rhombencephala were dissected at E15 or E16 and held in culture for up to 9 days. During the first 1 or 2 days in culture, the neurones had a round shape and started to proliferate and differentiate. As is shown in Fig. 2*A*, cell cultures contained morphologically different types of neurones which had been described as small bipolar, medium-sized fusiform or large multipolar (Törk, 1985). The most distinctive cells were the large multipolar neurones (Fig. 2*A*). From these large cells but also from other types of neurones, we were able to record erg currents. The most sTable patch-clamp recordings were obtained from neurones held in culture for 4–9 days. In large multipolar neurones (> 30 pF) erg currents were regularly recorded and in about half of the smaller neurones (< 30 pF) investigated an erg current was also present.

To increase the amplitude of the erg current and to suppress the activity of Ca^{2+} currents and Ca^{2+}-activated currents, the measurements were performed in an extracellular solution containing 40 mM K^+ with Ca^{2+} buffered to a nanomolar concentration. Figure 2 shows families of membrane currents elicited with a pulse protocol designed to detect native erg currents (Bauer *et al.* 1990; Schledermann *et al.* 2001; Sacco *et al.* 2003). The holding potential was −20 mV and each 1 s test pulse was preceded by a 2 s pulse to +20 mV to fully activate the erg channels (Shibasaki, 1987). Since erg channels inactivate faster than they activate, the amplitude of the erg current at the end of the conditioning depolarization was very small (Trudeau *et al.* 1995). Upon a strong hyperpolarizing test

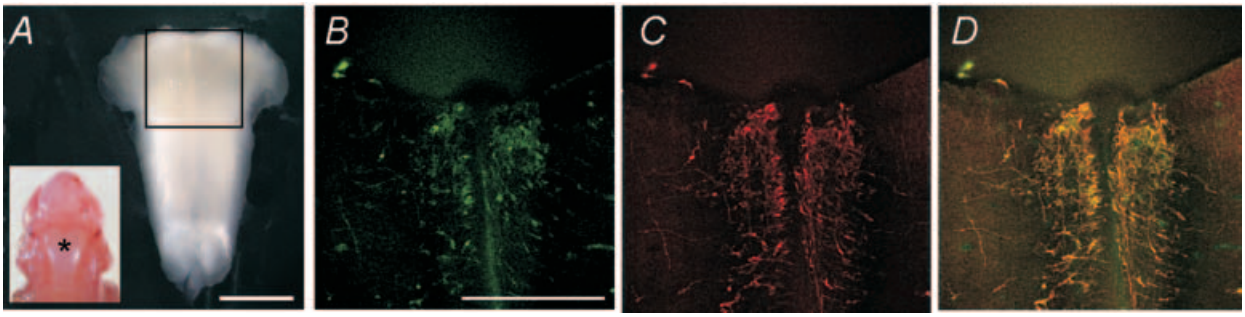

Figure 1. Embryonic raphe neurones stain for the erg1 channel protein and serotonin
A, the rhombencephalon after dissection from a rat embryo. Inset, dorsal view of a rat embryo (E15) with the asterisk (*) indicating the position of the rhombencephalon. *B–D*, area of the rhombencephalon as indicated by the black square in *A* after labelling with antibodies against erg1 (*B*) and serotonin (*C*). *D*, overlay of *B* and *C*. Serotonin and erg1 positive cells are located along the median line forming the raphe nucleus. This region was further dissected and dissociated for cell culture. Scale bars in *A*, 1 mm; *B–D*, 0.5 mm.

pulse to −120 mV, a transient inward current occurred which subsequently decreased to small values. This transient inward current was due to fast recovery from erg channel inactivation and subsequent slow deactivation of the erg channels. Since all erg channels were deactivated at the end of the 1 s test pulse to −120 mV, no erg current was recorded upon the final repolarizing pulse to −100 mV. With less negative test pulses transient tail currents were recorded, whose amplitude increased with less deactivation at the end of the preceding test pulse.

As explained above, the hook-like shape and the slow deactivation of the inward current pointed towards the presence of erg channels (Fig. 2*Ba*). After application of the antiarrhythmic substance E-4031 known to specifically block erg channels (Spector *et al.* 1996; Weinsberg *et al.* 1997), the transient inward currents were indeed totally blocked (Fig. 2*Bb*). The delayed outwardly rectifying current was not significantly affected by the drug. Nevertheless, in this experiment (Fig. 2*Bb*) there was a small unspecific increase in the delayed rectifying outward current elicited by the depolarization to 0 mV

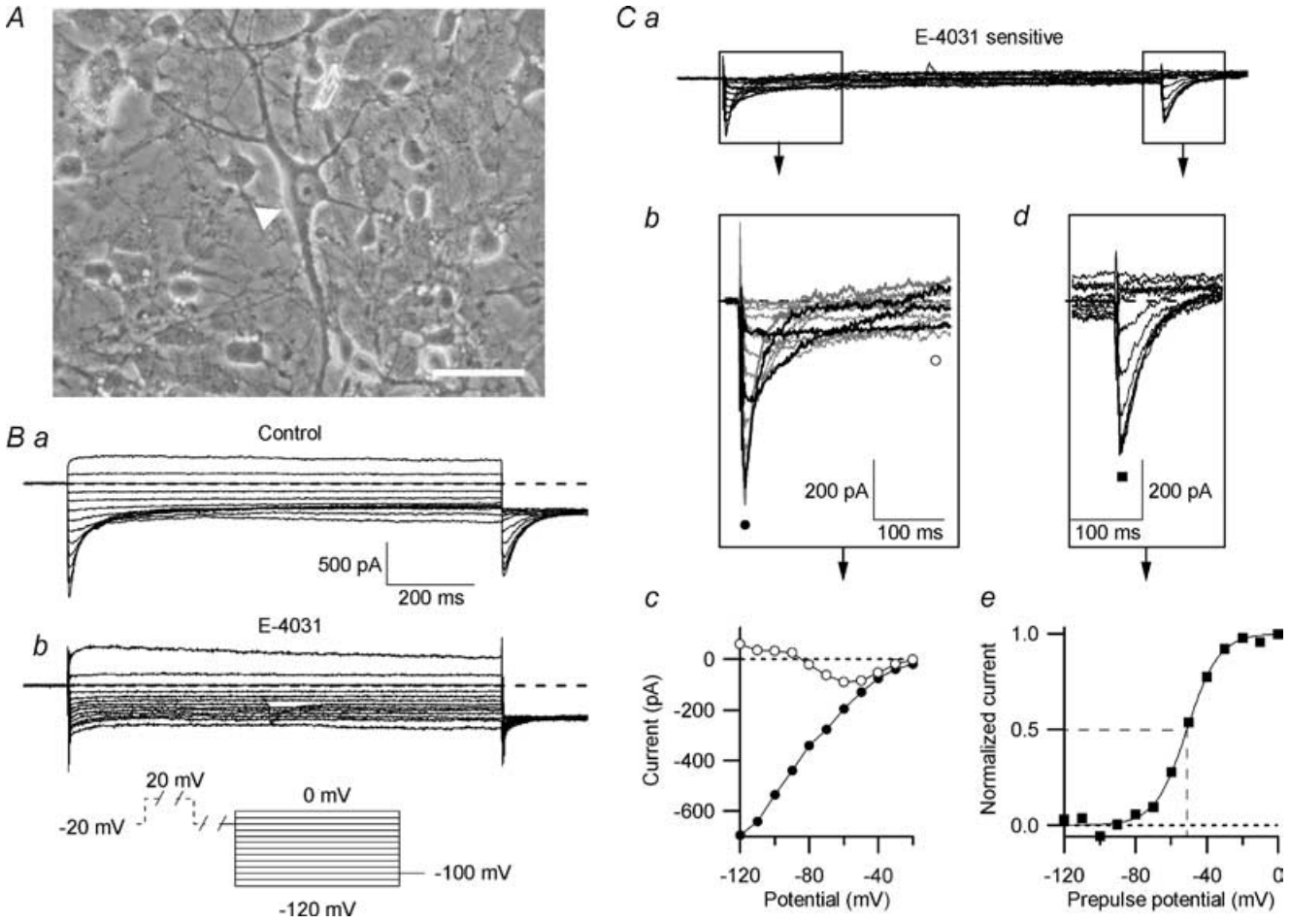

Figure 2. The E-4031-sensitive erg current in embryonic rhombencephalon neurones
A, photograph of a primary culture of rat embryonic rhombencephalon (E15) held in culture for 5 days. Neurones of various magnitude and shape were present. Predominantly, the large multipolar neurones (arrowhead) were chosen for this study. Scale bar: 40 μm. *Ba*, control currents recorded in 40 mM K^+ bath solution. From a holding potential of −20 mV, a 2 s pulse to 20 mV was applied, followed by a 500 ms gap at −20 mV, 1 s test pulses to potentials between 0 and −120 mV in steps of 10 mV and a final 200 ms potential step to −100 mV (see pulse diagram). *Bb*, same cell and pulse protocol as in *B*, but in the presence of 10 μM E-4031. *Ca*, E-4031-sensitive current, obtained by subtracting the current traces shown in *Bb* from those shown in *Ba*. *Cb*, the beginnings of the enlarged E-4031-sensitive current traces are depicted. Highlighted in black are current traces recorded at −50, −80 and −110 mV, demonstrating the characteristic potential-dependent time courses of recovery from inactivation and subsequent deactivation of erg currents. *Cc*, peak inward current amplitudes (●) and current amplitudes at 250 ms (○) plotted *versus* the test pulse potential. *Cd*, tail currents from *Ca* on enlarged coordinates. The peak current amplitudes were plotted against prepulse potential, and a Boltzmann function was fitted to the data points (*Ce*) with $V_{1/2} = -51.4$ mV and the slope factor $k = 8.7$ mV.

after application of E-4031. E-4031-sensitive currents were obtained by subtracting the corresponding membrane current traces before and after application of E-4031 (Fig. 2*Ca*). On expanded coordinates the time course of the transient inward currents elicited by the hyperpolarizing test pulses is more clearly seen, especially the strong voltage dependence of the time course of recovery from inactivation and subsequent deactivation (Fig. 2*Cb*). The current–potential relation of the E-4031-sensitive peak-current amplitude demonstrated the pronounced inward rectification of the erg currents (Fig. 2*Cc*). The current amplitudes at 250 ms plotted *versus* membrane potential showed that deactivation was not complete between −50 mV and −80 mV, whereas at more negative potentials, the erg current was fully deactivated. Close to the calculated reversal potential for K^+, which is −34 mV in these experiments, the erg current amplitude decreased. The amplitude of the E-4031-sensitive current elicited upon the constant −100 mV pulse consisted of an instantaneous current component whose amplitude corresponded to the fraction of open channels at the end of the preceding test pulses, as well as of a current component due to recovery from inactivation which proceeded fast at −100 mV (Fig. 2*Cd*). The tail currents were normalized to the maximal erg inward current and plotted *versus* prepulse potential (Fig. 2*Ce*). The data points were fitted by a Boltzmann function characterizing the voltage dependence of the erg channel availability.

In almost all large multipolar neurones an erg current was recorded, whereas it was found in only about 50% of other types of primary cultured rhombencephalon neurones. Generally, small neurones with few and thin dendrites tended to have no erg current. Since we observed that the amplitudes of the erg currents increased with the time in culture, we investigated whether this corresponded to an increase in the erg current density. The cell capacitance (C_{slow}) was taken as a measure for the cell size, and the current amplitudes were obtained from Boltzmann fits to the voltage dependence of the maximal tail current amplitudes as shown in Fig. 2*Ce*. Because the cells proliferated over time in culture, the cell capacitance of the measured cells increased from 10 ± 1 pF on day 1 in culture ($n = 11$) to 57 ± 17 pF on day 8 in culture ($n = 5$). Despite this increase in the size of the recorded cells, the erg current density remained almost constant, slightly rising from 6.2 ± 1.1 pA pF^{-1} to 8.3 ± 1.4 pA pF^{-1}, respectively. This difference was not statistically significant. The erg current density of all neurones measured at different times in culture ($n = 66$) ranged from 2 to 24 pA pF^{-1}, with an average of 7.7 ± 0.6 pA pF^{-1}. Since the largest amplitudes of the erg current were recorded from large multipolar neurones (30–130 pF), similar to the one shown in Fig. 2*A*, we decided to preferably record from these cells. We found no significant differences between the biophysical properties of the erg currents from these large multipolar neurones and other rhombencephalon neurones. Similarly, there were no differences between the erg currents recorded from neurones at different times in culture. Therefore the results described below contain data pooled from all days and all cell sizes.

Serotonergic neurones express different erg subunits

To study the molecular identity of the channels mediating the neuronal erg current, single-cell RT-PCR was performed in neurones from rhombencephala cultured for 6–9 days (Fig. 3) with and without prior patch-clamp recording. Primers for erg1 (or alternatively for the splice variants erg1a or erg1b), erg2 and erg3 were used. We also studied the presence of transcripts for neuronal tryptophan hydroxylase (TPH2; Walther & Bader, 2003) to identify serotonergic neurones. Primers for the glial fibrillary acidic protein (GFAP), the main component of the astrocyte intermediate filament cytoskeleton (Eng *et al.* 2000), were used to identify astrocytes chosen by accident. Two cells were positive for GFAP and excluded from the further evaluation. This is important since erg1 channels have been shown to be expressed in hippocampal astrocytes (Emmi *et al.* 2000).

Single-cell RT-PCR was performed from the cytoplasm of large multipolar neurones (> 30 pF) after a short recording protocol to confirm the presence of erg currents. In the multiplex PCR two different sets of primers were used. In the first set, cells were tested for erg1a, erg2, erg3, TPH2 and GFAP (Fig. 3*A*). In the second set, primers specific for erg1b instead of erg1a were used (Fig. 3*B*). The neurones tested in the first set ($n = 8$) contained transcripts for erg1a (88%), erg2 (0%), erg3 (50%), and TPH2 (63%). In the second set of experiments ($n = 16$) transcripts were detected for erg1b (25%), erg2 (31%), erg3 (94%), and TPH2 (100%). In summary, 88% of these large neurones possessing erg current ($n = 24$) were TPH2-positive indicating that these neurones were serotonergic. We found different combinations of erg channel subunits in individual cells. There was no obvious correlation between the presence or absence of a particular erg channel subunit and the apparent time course of erg current deactivation. However, no detailed analysis, e.g. of erg current kinetics was possible, since the pulse protocol applied prior to the harvesting of the cytoplasm was short and consisted of only 100 ms pulses to potentials between −90 and −120 mV.

A high percentage presence of TPH2 (90%) was also found in large multipolar neurones which were not patch-clamped before harvesting the cytoplasm ($n = 20$). Combining the results of all TPH2-positive cells ($n = 39$), the prevalent channel subunits were erg3 (82%, tested in 39 neurones), erg1 (78%, tested in 9 neurones with primers not distinguishing between erg1a and erg1b) and its splice variant erg1a (100%, tested in 5 neurones). Less frequently

erg1b (40%, tested in 25 neurones) and erg2 channel subunits (28%, tested in 39 neurones) were found. In only 5% of the TPH2-positive cells no mRNA for erg channel subunits was detected. In most large cells where no transcripts for TPH2 were found (4 of 5), mRNA for at least one erg subunit was detected.

PCR was also performed with cDNA from rat embryonic rhombencephalon cultures (E15) grown for 2 or 8 days. Transcripts for erg1, erg1b, erg2 and erg3 channel subunits, as well as for TPH2 and GFAP were tested separately (data not shown). The presence of transcripts for GFAP indicated that the cultures contained mature astrocytes at both times in culture. After 2 and 8 days in culture, transcripts for erg1subunits, TPH2 and GFAP were already found in the first round of PCR amplification. Transcripts for erg1b, erg2 and erg3 channel subunits could only be detected after the second round of PCR amplification.

Immunochemistry of embryonic rhombencephalon neurones

Because of the regular occurrence of neuronal TPH2 mRNA in cultured neurones, we tried to stain embryonic rhombencephalon neurones with an antibody against TPH. Six of nine neurobiotin-labelled large, multipolar neurones from which an erg current was recorded were clearly stained with the TPH antibody (Fig. 4). This result was confirmed in an additional group of large multipolar neurones (19/20) without previous patch-clamp recording.

Since there are contradictory reports about the presence of the erg1b channel subunit at the protein level in the brain, we performed Western blots (Fig. 5.) again using the antibody against erg1 described by Pond *et al.* (2000). Since this antibody is directed against a distal C-terminal peptide fragment of erg1, it should detect both the erg1a and erg1b channel subunits. Membrane preparations from CHO cells transfected with erg1a and the shorter N-terminal splice variant erg1b were used as positive controls and as markers for the expected position of the proteins on the gel. We then tested membrane preparations of whole adult rat brain and embryonic rhombencephalon (E16) to determine the protein size of native erg1 subunits, because in expression systems like CHO cells proteins are often not fully glycosylated. Additionally, we used membrane preparations of the pituitary and the lactotrope cell line MMQ which is known to contain an endogenous

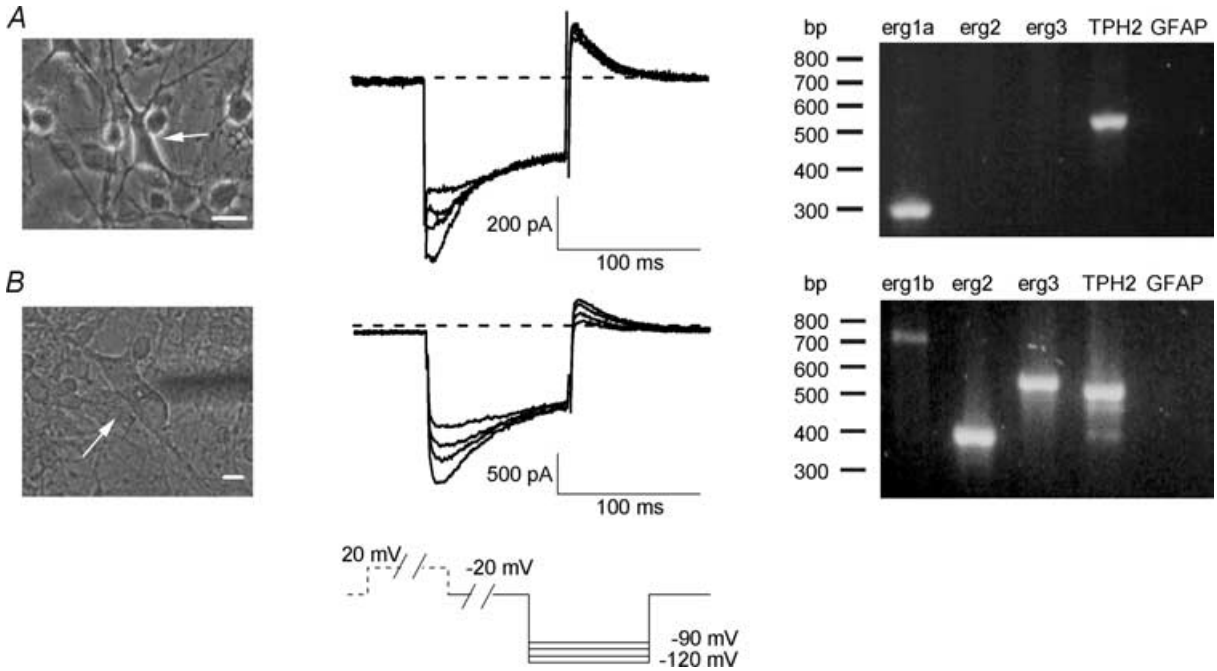

Figure 3. Transcripts for different erg channels are present in embryonic rhombencephalon neurones as revealed by single-cell RT-PCR

Brief electrophysiological recordings in 40 mM K^+ bath solution were performed prior to single-cell RT-PCR. Voltage pulse protocol shown at the bottom. Holding potential was −20 mV. Erg currents were activated by a voltage pulse to +20 mV for 2 s and inward currents were elicited by 100 ms pulses to potentials from −90 to −120 mV in steps of 10 mV. Erg currents were identified by the typical hook-like shape. *A*, large, multipolar neurone (left, arrow) from which transient inward currents typical for the presence of erg current were recorded (centre). Single-cell RT-PCR for this cell (right) in which erg1a and TPH2 were found. *B*, large, multipolar neurone (left, arrow) from which an erg current was recorded (centre). Transcripts for all three tested erg channel subunits were found in this cell (right). The absence of glial fibrillary acidic protein (GFAP), normally present in astrocytes, served as a negative control. Scale bars: 10 μm.

erg current (Schäfer *et al.* 1999; Lecchi *et al.* 2002). In preparations of CHO cells transfected with erg1a or erg1b cDNA, single protein bands at the expected sizes of partially glycosylated channel subunits (~140 kDa and ~95 kDa, respectively) were found. In membrane preparations from cultured embryonic rhombencephalon, pituitary, MMQ cells and whole brain membrane preparations unglycosylated and glycosylated proteins of the erg1 subunit (~130 kDa and ~160 kDa) and a smaller protein, probably representing glycosylated protein of the erg1b subunit (~100 kDa), were detected. In conclusion, our experiments show that the erg1b channel subunit protein is indeed present in the adult rat brain and embryonic rhombencephalon. Whereas in the whole brain the expression of erg1b was clearly weaker than erg1a, it was similar in the rhombencephalon. However, there was also a ~200 kDa protein band in all of these tissues. This large protein which was also found by Pond *et al.* (2000) in their Western blots cannot be attributed to any known erg protein. This imposes some limitations on the interpretation of the staining for erg1 shown in Fig. 1.

Comparison of neuronal with heterologously expressed erg channels

Since we detected the transcripts for all three erg channel subunits as well as that of the splice variant erg1b, it is possible that all of these erg subunits may take part in the formation of the erg channels in raphe neurones. To narrow down the molecular identity of the erg channels in serotonergic neurones we compared the biophysical properties of the endogenous erg current with those mediated by the two splice variants of erg1 (erg1a and erg1b) as well as erg2 and erg3 channels after heterologous expression in CHO cells using the identical pulse protocols and solutions. The biophysical properties of the currents mediated by the heterologously expressed rat erg channels were in accordance with previous results (erg1–3: Shi *et al.* 1997; Schledermann *et al.* 2001; Wimmers *et al.* 2001; erg1b: Lees-Miller *et al.* 1997; London *et al.* 1997).

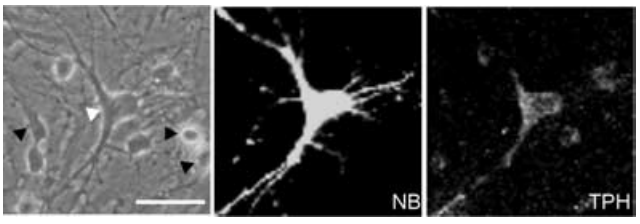

Figure 4. Presence of TPH in large rhombencephalon neurones with erg current
An erg current was recorded in a large multipolar embryonic rhombencephalon neurone (left, white arrowhead) with neurobiotin included in the pipette solution. The neurobiotin-filled neurone (centre, NB) was additionally immunostained with an antibody against tryptophan hydroxylase (right, TPH). Black arrowheads indicate TPH-negative cells. Scale bar: 40 μm.

Voltage dependence of erg current availability

The voltage dependence of erg current availability was determined with the same pulse protocol as that described in Fig. 2. The fraction of erg channels available at the end of the 1 s test pulses was determined with a constant pulse to −100 mV. The amplitude of these tail currents was a measure of the potential-dependent availability of erg channels. In raphe neurones membrane currents were recorded before and after application of E-4031. Figure 6 shows the E-4031-sensitive currents obtained in a raphe neurone (Fig. 6*A*) and membrane currents measured in CHO cells after expression of erg1a (Fig. 6*B*), erg1b (Fig. 6*C*), erg2 (Fig. 6*D*) and erg3 (Fig. 6*E*). Comparison of the five current families showed that erg1a and erg2 currents exhibited much slower deactivation kinetics than the neuronal erg currents and erg1b and erg3 currents. The peak amplitudes of the transient inward currents recorded at the constant pulse to −100 mV were normalized, plotted *versus* the prepulse potential and fitted with Boltzmann functions (Fig. 6*F*). The midpoint potential of the availability curve ($V_{1/2}$) of the endogenous erg current was similar to that of erg3 currents, whereas $V_{1/2}$ of the three other erg currents was located either at about 20 mV more negative (erg1a and erg2) or more positive potentials (erg1b; see also Table 1). The location of $V_{1/2}$

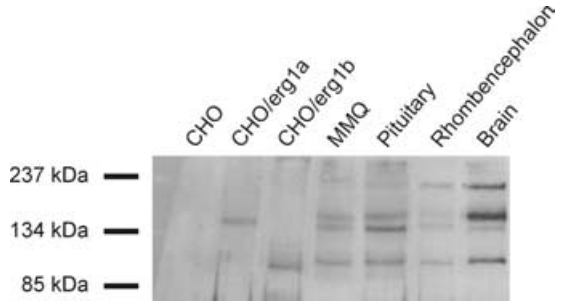

Figure 5. Different erg1 splice variants are expressed in rhombencephalon as revealed by Western blot
Immunoblots of membrane preparations of untransfected CHO cells, CHO cells transiently expressing erg1a or erg1b channels, lactotrope MMQ cells, rat pituitary, rat embryonic rhombencephalon and adult rat brain. An antibody against the erg1 C-terminus was used. There was no staining in untransfected CHO cells. The antibody detected proteins in CHO cells expressing erg1a or erg1b at positions expected for erg1a and erg1b. Proteins close to the size of erg1a in CHO cells were found in MMQ cells, pituitary, rhombencephalon and brain. The bands with slightly higher molecular mass probably represent the glycosylated proteins. Proteins close to the size of erg1b in CHO cells were found in MMQ cells, pituitary, rhombencephalon and brain, representing glycosylated forms of erg1b. In addition, in MMQ cells, pituitary, rhombencephalon and brain the antibody stained a high molecular mass protein (~200 kDa) of unknown origin.

of erg1a and erg2 availability curves at apparently more negative potentials is at least partially due to their much slower time course of deactivation (Fig. 6*B* and *D*) than that of the neuronal erg current, because at the end of the 1 s variable test pulses, deactivation did not reach a steady-state. The slope factors of the Boltzmann fits of the erg availability curves in rhombencephalon neurones did not differ significantly from those of heterologously expressed erg1a and erg2 channels (Table 1).

Time constants of erg current deactivation

The majority of erg currents recorded from embryonic rhombencephalon neurones showed a remarkably similar voltage-dependent time course of deactivation during the hyperpolarizing pulses. Due to the small density of the neuronal erg currents and thus a low signal-to-noise ratio, the decaying portion of the native erg inward current was fitted with only one single exponential function. Erg currents were elicited by the availability protocol (see Fig. 6). The neuronal E-4031-sensitive currents were analysed and compared to the erg currents measured after heterologous expression of the different erg channels (Fig. 6). Since the time course of deactivation of the heterologously expressed erg currents often was better fitted with two than with one exponential function, only the period at the beginning of current deactivation which mainly represented the fast deactivating component was fitted with a single exponential function (Fig. 7*A*). The fitted current segment was adjusted for each voltage,

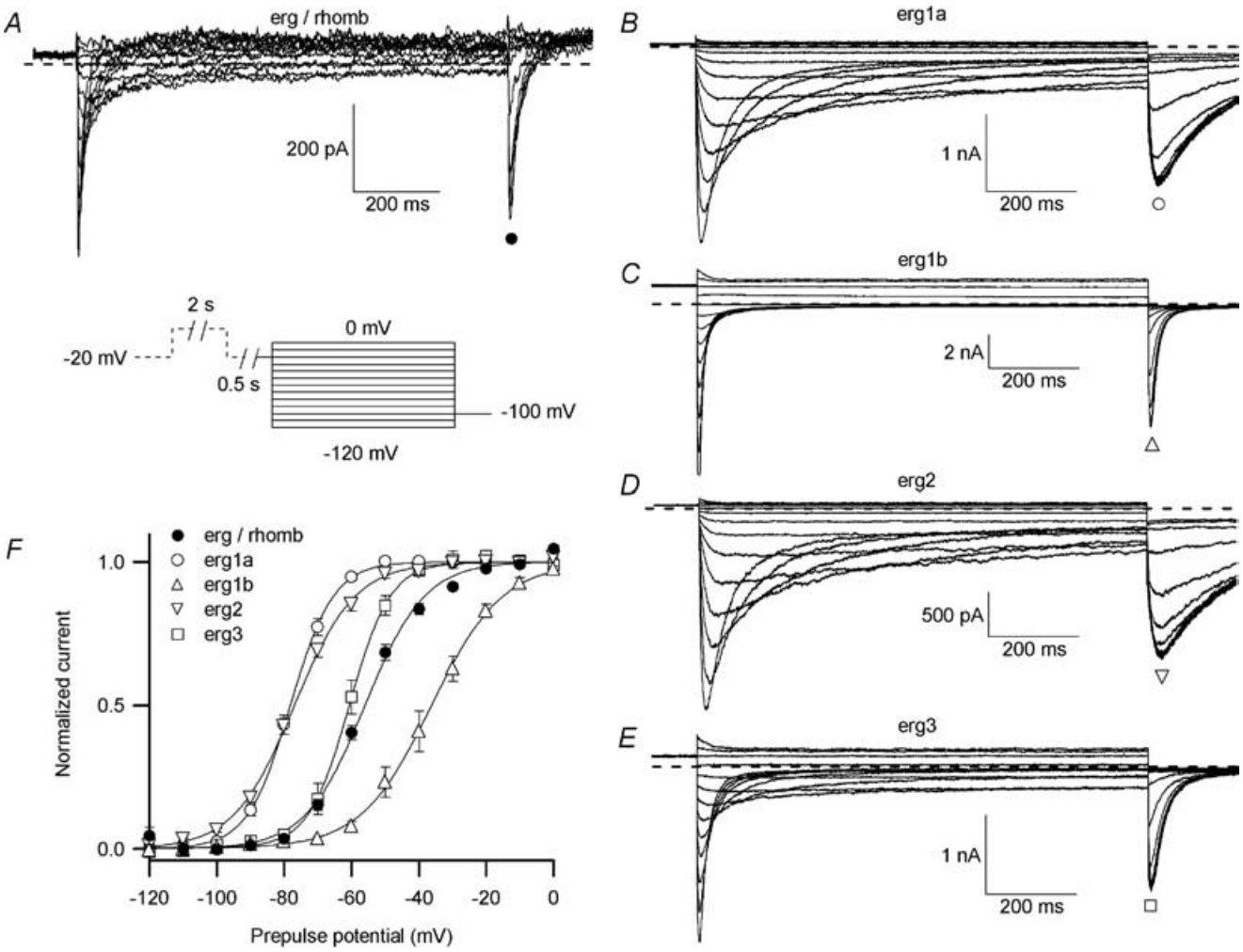

Figure 6. Voltage dependence of erg current availability
Comparison of neuronal erg current measured in embryonic rhombencephalon neurones with erg currents in CHO cells after expression of different erg channel subunits, recorded with identical solutions and pulse protocols (see pulse diagram). *A*, E-4031-sensitive currents recorded in a rhombencephalon neurone. Families of erg currents measured after heterologous expression of erg1a (*B*), erg1b (*C*), erg2 (*D*) and erg3 (*E*) channels in CHO cells. *F*, means of the normalized peak tail current amplitudes of erg currents recorded in rhombencephalon neurones (●; $n = 55$), as well as of erg1a (○; $n = 6$), erg1b (Δ; $n = 8$), erg2 (∇, $n = 10$) and erg3 (□; $n = 5$) currents in CHO cells plotted *versus* the test pulse potential. Data were fitted with a single Boltzmann function. The mean values for $V_{1/2}$ and the slope factor k of the individual Boltzmann functions are collected in Table 1.

Table 1. Midpoint potentials and slope factors of isochronal availability and activation curves of native erg current from rat embryonic rhombencephalon neurones and heterologously expressed erg currents

	$V_{1/2}$ (mV)	*P*	*k*	*P*	*n*
Availability curves, fast deactivation only					
Erg/rhomb	−56 ± 1	—	8.7 ± 0.4	—	55
Erg1a	−78 ± 1	***	6.3 ± 0.3	ns	6
Erg1b	−36 ± 2	***	9.7 ± 1.0	ns	8
Erg2	−77 ± 1	***	8.9 ± 0.4	ns	10
Erg3	−61 ± 1	ns	6.1 ± 1.0	ns	5
Availability curves, fast and slow deactivation					
Fast and slow deactivation					
Erg/rhomb	− 57 ± 2	—	9.9 ± 1.6	—	6
	−110 ± 2	—	4.2 ± 0.5	—	—
Slow deactivation, only					
Erg/rhomb	−105 ± 4	—	9.4 ± 2.1	—	5
Activation curves					
Erg/rhomb	−42 ± 1	—	8.0 ± 0.6	—	10
Erg1a	−37 ± 3	ns	7.6 ± 0.2	ns	6
Erg1b	−40 ± 2	ns	9.2 ± 0.6	*	20
Erg2	−3 ± 1	***	6.6 ± 0.3	ns	6
Erg3	−54 ± 1	***	5.4 ± 0.4	**	12

Erg/rhomb are data from erg currents of rat embryonic rhombencephalon neurones; erg1a, erg1b, erg2 and erg3 are data from CHO cells expressing the different erg channel subunits. $V_{1/2}$, midpoint potentials of availability and activation curves obtained from Boltzmann fits. In 5 neurones exclusively exhibiting a slowly deactivating erg current component with a negative voltage dependence, $V_{1/2,\text{slow}}$ was determined by a single Boltzmann function. If erg current in neurones had two voltage dependencies ($n = 6$), $V_{1/2,\text{fast}}$ and $V_{1/2,\text{slow}}$ were taken from the sum of two Boltzmann fits as in Fig. 8*B*. In this case $V_{1/2,\text{fast}}$ corresponded to $V_{1/2}$. *k*, slope factors of the respective Boltzmann fits. Values are means ± S.E.M. Data from erg channels expressed in CHO cells were tested against native erg with Student's two-tailed unpaired *t* test. Significance indicated by: $^{*}P \leq 0.05$; $^{**}P \leq 0.01$; $^{***}P \leq 0.001$; ns, not significant.

because the time constants of recovery from inactivation and of deactivation became smaller at more negative potentials. Once the current segment was chosen it was kept constant for all analysed currents at a given potential. The current segments were from 10 to 100 ms of the 1 s potential step to −120 mV and increased to a current segment from 30 to 350 ms at −70 mV. The data collected in Fig. 7*C* show that the time constants of deactivation of the native erg current resembled most closely those found for erg3 currents. In contrast, erg1b currents deactivated significantly faster, and erg1a and erg2 currents deactivated significantly slower than the native erg current.

Slowly deactivating erg current component

A small population of rhombencephalon neurones (17%) exhibited a slowly deactivating erg current component. In about half of these neurones (5 of 11) deactivation proceeded exclusively slowly, whereas in the other six neurones both deactivating components were present. Depending on the incidence of one or two components, the availability curves measured in these neurones were fitted with either one or the sum of two Boltzmann functions. In the example of Fig. 8*A*, membrane current traces were superimposed, the traces recorded by test pulses to −60, −90 and −120 mV were set off in black. Whereas in most raphe neurones deactivation of the erg current was complete at −90 mV (see Fig. 6*F*), the current trace at −90 mV in Fig. 8*A* demonstrated incomplete deactivation resulting in a considerable tail current amplitude. Only with the stronger negative pulse to −120 mV deactivation was almost complete. The data points had to be fitted with the sum of two Boltzmann functions yielding a bimodal availability curve (Fig. 8*B*). In this and the five similar experiments, the midpoint potential of the slowly deactivating component was located at a very negative potential ($V_{1/2,\text{slow}} = -110$ mV), whereas the midpoint potential of the fast deactivating component

($V_{1/2,\text{fast}} = -57$ mV) had a similar value as that determined for erg currents of the majority of rhombencephalon neurones ($V_{1/2} = -56$ mV). $V_{1/2}$ of the five neurones with an exclusively slowly deactivating erg current was −105 mV. The data are summarized in Table 1. The slowly deactivating current component was reminiscent of erg currents so far only described in rat native lactotropes (Schäfer *et al.* 1999) and in the lactotrope MMQ cell line (Lecchi *et al.* 2002).

Voltage dependence of erg current activation

The voltage dependence of activation was measured from a holding potential of −80 mV at which erg channels are completely deactivated. To activate the erg channels, the cells were depolarized with 4 s test pulses which increased in amplitude in intervals of 10 mV. At the end of the variable test pulses the fraction of activated channels was measured with a constant pulse to −100 mV. The different erg currents shown in Fig. 9*A*–*E* demonstrate their inwardly rectifying properties. The normalized tail current amplitudes were plotted *versus* test pulse potential in Fig. 9*F*. The midpoint potential of erg channel activation for the native erg current was not significantly different from the heterologously expressed erg1a and erg1b channels (see Table 1). The voltage dependencies of erg2 and erg3 channel activation were at an about 40 mV more positive or an about 10 mV more negative membrane potential, respectively. The $V_{1/2}$ values obtained for the isochronal activation of erg1a and erg2 channels differ substantially from those of the availability curves (Fig. 6). The difference can be explained by the very slow time courses of activation (Fig. 9) and deactivation (Fig. 7). The midpoint potentials would coincide if sufficiently long prepulse durations were applied to reach steady-state conditions (Schönherr *et al.* 1999). However, such an experimental protocol is hampered by the fragile nature of the recordings in raphe neurones. In contrast, activation and availability midpoint potentials were very similar for erg1b and erg3 channels (see Table 1) which activate and deactivate relatively fast (see Fig. 7), and therefore steady-state conditions were approximately achieved.

Time course of erg current activation

The time constants of activation of the neuronal erg current as well as that of erg1a, erg1b, erg2 and erg3 currents after heterologous expression were determined

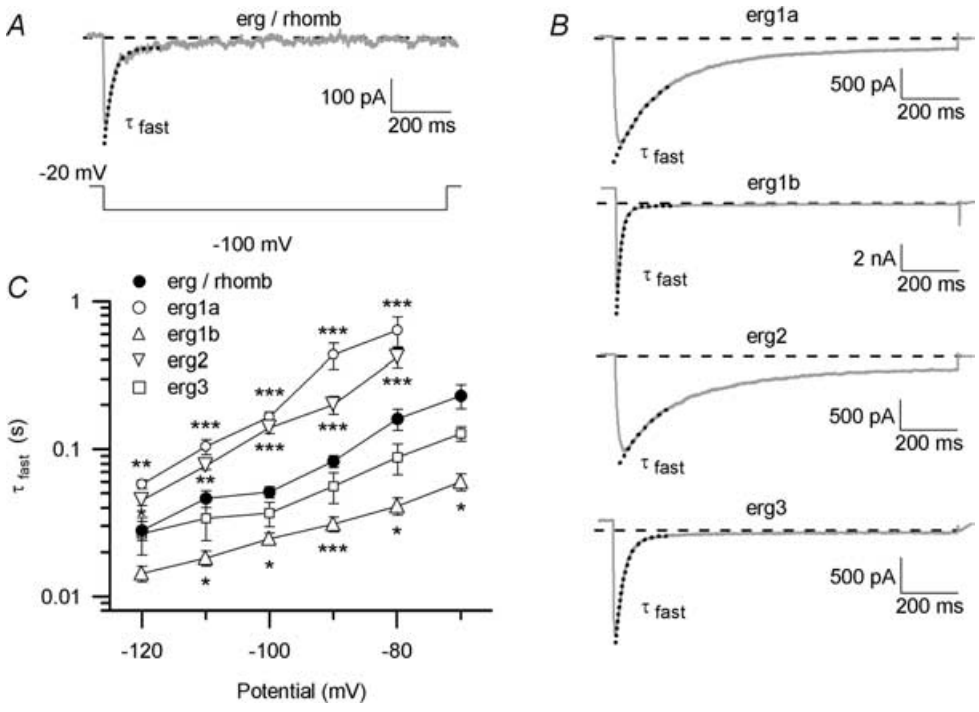

Figure 7. Time course of fast erg current deactivation
E-4031-sensitive currents measured in a rhombencephalon neurone and erg currents following heterologous expression of erg1a, erg1b, erg2 and erg3 channels in CHO cells were recorded with the pulse protocol as described in Figs 2 and 6. The deactivating erg currents elicited by the test pulses between −70/−80 mV and −120 mV were fitted with a single exponential function to the fast decaying part of the curves (dotted lines in *A* and *B*) yielding the time constant τ_{fast}. Example traces elicited by the test pulse to −100 mV of native (*A*) and heterologously expressed currents (*B*). *C*, mean values of time constants τ_{fast} of deactivation plotted against the test potential for erg currents in rhombencephalon neurones (●; $n = 24$), as well as for erg1a (○; $n = 6$), erg1b (Δ; $n = 8$), erg2 (∇; $n = 10$) and erg3 (□; $n = 5$) currents measured in CHO cells. Asterisks indicate significance against τ_{fast} of rhombencephalic erg (*$P \leq 0.05$; **$P \leq 0.01$; ***$P \leq 0.001$).

with an envelope-of-tail protocol (see Wang *et al.* 1997). From a holding potential of −80 mV a depolarizing pulse to +20 mV of increasing duration was applied, the time course of erg current activation was then traced with the amplitude of the tail current elicited with a pulse to −100 mV (Fig. 10). The increase in the tail current amplitudes plotted against prepulse duration could be fitted with a single exponential function yielding the time constants of erg current activation at 20 mV. While the time course of activation of the native erg current ($\tau_{\text{activation}} = 123 \pm 20$ ms, $n = 7$) was similar to that of erg1b ($\tau_{\text{activation}} = 106 \pm 11$ ms, $n = 11$) and erg3 currents ($\tau_{\text{activation}} = 95 \pm 6$ ms, $n = 4$), it was slower for the current activation mediated by erg1a and erg2 channels ($\tau_{\text{activation}} = 215 \pm 46$ ms, $n = 5$ and 821 ± 53, $n = 9$, respectively). However, the difference between the time course of activation of the native erg current and that of the erg1a current did not reach statistical significance (Fig. 10*F*).

Discussion

Erg currents were recorded in rat embryonic rhombencephalon neurones. Most of these neurones were serotonergic as revealed by the presence of neuronal tryptophan hydroxylase (TPH2; Walther & Bader, 2003). The electrophysiological properties of the neuronal erg current were relatively homogeneous and characterized by fast activation and deactivation kinetics. Single cell RT-PCR showed that in individual neurones various combinations of erg subunits can be expressed. The biophysical properties of the neuronal erg current were in between those of the different heterologously expressed erg currents. These results suggest that the erg current in rat embryonic rhombencephalon neurones are mediated by heteromeric erg channels.

Expression of erg current in serotonergic neurones

Using RT-PCR in rhombencephalic cell cultures we found the transcripts for erg1a, erg1b, erg2 and erg3. Our single cell RT-PCR data show that these erg subunits were expressed in different combinations in large multipolar raphe neurones. These neurones were serotonergic because they regularly expressed the neuronal isoform of tryptophan hydroxylase (TPH2). TPH2 is a key enzyme for the synthesis of serotonin (Grahame-Smith, 1964) and is predominantly expressed in raphe nuclei, whereas the other isoform (TPH1) is expressed in the gut and pineal gland (Patel *et al.* 2004). These results confirm and extend previous findings obtained by *in situ* hybridization that the three members of the erg K^+ channel subfamily are differentially expressed in rat brain (Saganich *et al.* 2001; Papa *et al.* 2003). In these studies, erg1 and erg3 (Saganich *et al.* 2001) or all three erg channels (Papa *et al.* 2003) have been found in brainstem nuclei of adult rat, among them the raphe nuclei. Also in embryonic mouse brain (E9.5) all three erg mRNAs are present throughout the brain changing to a more differentiated expression at E13.5 (Polvani *et al.* 2003).

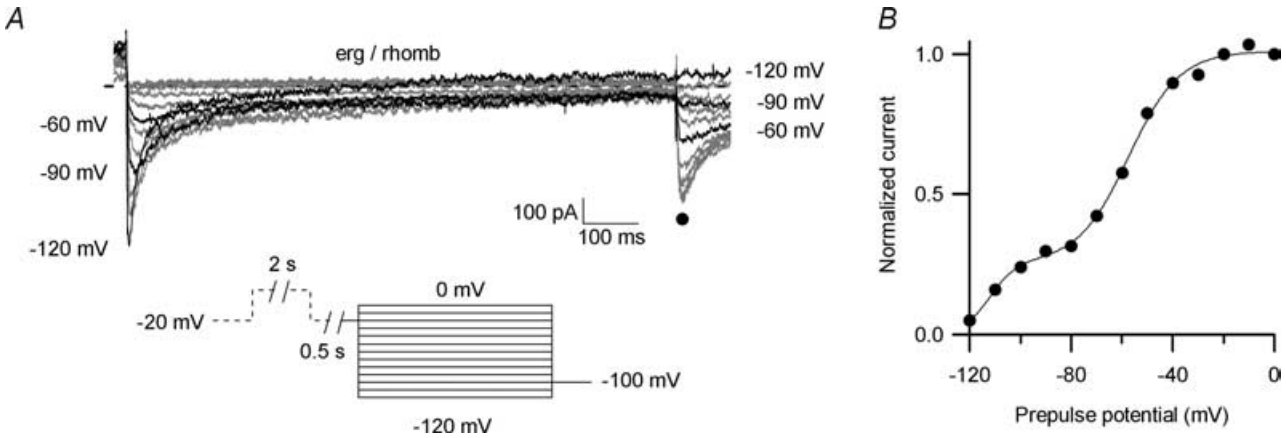

Figure 8. A slowly deactivating erg current component occurs in a subpopulation of rhombencephalon neurones

Erg current availability measured in an embryonic rhombencephalon neurone using the same pulse protocol as in Fig. 2 (see pulse diagram). *A*, E-4031-sensitive current from a rhombencephalon neurone with a fast and a slowly deactivating erg current component. Current traces recorded with test pulses to −60, −90 and −120 mV shown in black. *B*, normalized peak tail current amplitudes of the E-4031-sensitive current shown in *A* plotted *versus* prepulse potential. Data points were fitted with the sum of two Boltzmann functions. The slowly deactivating erg current component was described by $V_{1/2} = -112$ mV and a slope factor of $k = 5$ mV and the fast deactivating current component by $V_{1/2} = -57$ mV and a slope factor of 10 mV. The relative contribution of the slowly deactivating current component to the total current amplitude in this neurone was 0.25.

Biophysical properties of the neuronal erg current

The single-cell RT-PCR data show that serotonergic neurones can express all three erg subunits. The Western blots demonstrate that the erg1a and erg1b subunit proteins are indeed present in the raphe cell culture. The heterologously expressed erg currents mediated by the various erg subunits detected in raphe neurones exhibit most remarkable differences concerning their gating kinetics: erg1b and erg3 channels activate and deactivate considerably faster than erg1a and erg2 channels (erg1–3: Shi *et al.* 1997; Wimmers *et al.* 2001; erg1b: Lees-Miller *et al.* 1997; London *et al.* 1997). Our present experiments in CHO cells including the data on the newly cloned rat erg1b are in full agreement with these previous results.

The coexpression of several erg subunits in individual serotonergic neurones as well as the finding that the voltage- and time-dependent properties of the neuronal erg current share different aspects of erg1a, erg1b and erg3 currents (see Table 1), suggest that it is presumably mediated by heteromeric erg channels. We have recently shown that erg1–3 subunits can indeed form heteromeric channels (Wimmers *et al.* 2001). Some of the biophysical properties of heteromeric erg channels like the voltage dependence of current activation are in between those

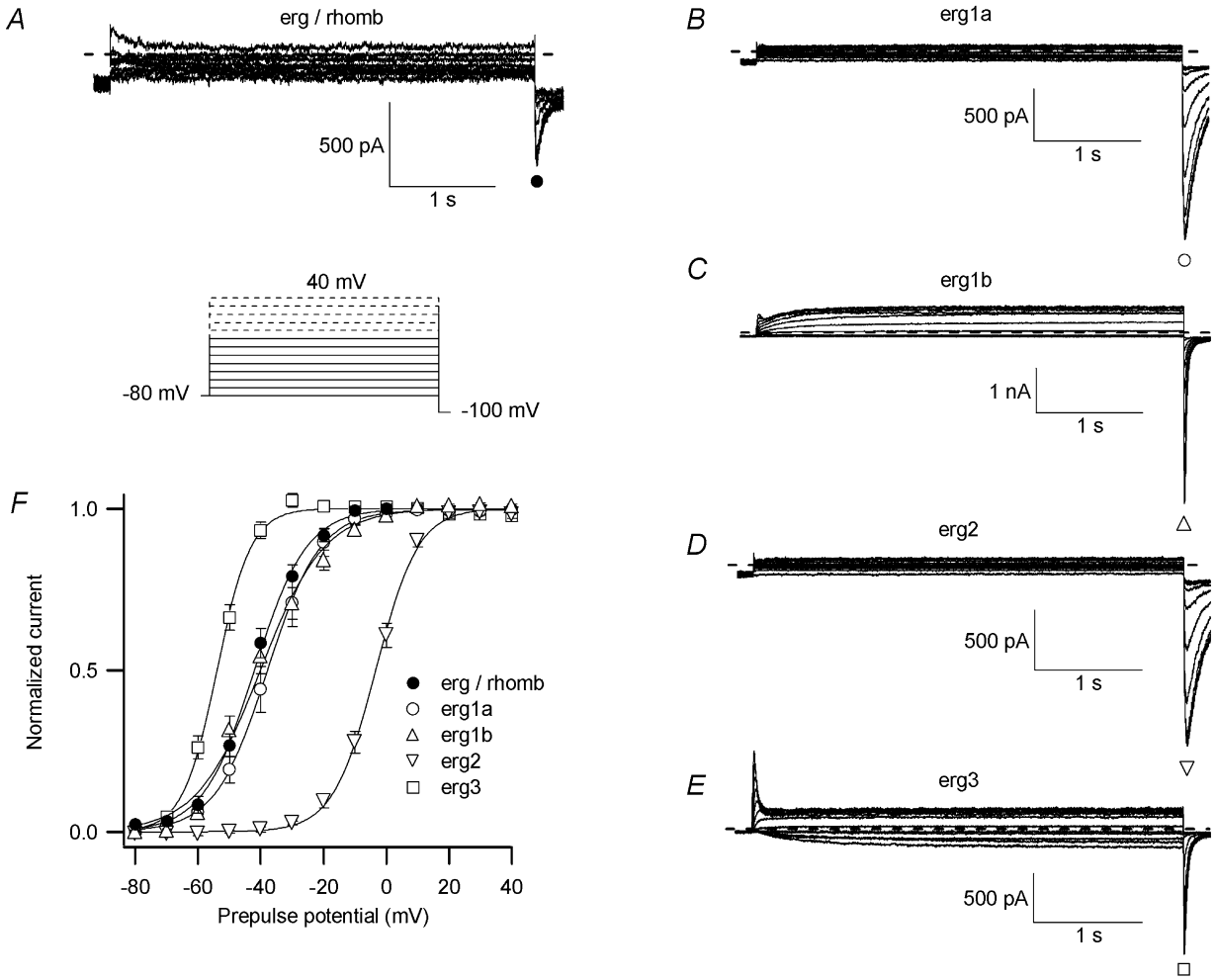

Figure 9. Voltage dependence of erg current activation
A, E-4031-sensitive current measured in an embryonic rhombencephalon neurone to compare the neuronal erg current activation with that of erg1a (*B*), erg1b (*C*), erg2 (*D*) and erg3 (*E*) currents in CHO cells after expression of the different erg channels. The transient outward current shown in *A* is presumably a rundown artefact of an A-type current. The voltage dependence of activation was determined from a holding potential of −80 mV. Inward currents were elicited by a constant pulse to −100 mV following 4 s prepulses to potentials between −80 and 40 mV in steps of 10 mV to activate erg currents (see pulse diagram). The neuronal inward erg currents following the prepulses from 10 to 40 mV (dashed lines in pulse diagram) were omitted from the analysis, because they often were biased by rundown of other tail currents. *F*, means of normalized peak tail current amplitudes of rhombencephalic erg current (●; $n = 10$), as well as of erg1a (○; $n = 6$), erg1b (△; $n = 20$), erg2 (▽; $n = 6$) and erg3 (□; $n = 12$) currents plotted against the prepulse potential.

of the corresponding homomeric erg channels, while the activation kinetics are dominated by the 'faster' erg channel subunits (Wimmers *et al.* 2002). The erg current in raphe neurones has properties akin to those mediated by heteromeric channels: its voltage dependence of activation is in between that of homomeric erg3 and that of erg1a and erg2 currents. In addition, its activation kinetics are faster than those of erg2 and erg1a currents, but similar to those of the 'fast' erg1b and erg3 currents. The eactivation time course of the neuronal current is also significantly faster than that of the erg1a and erg2 currents, but similar to that of erg3 currents. Only erg1b currents deactivate faster. Since in the majority of the serotonergic neurones erg1a and erg3 channel subunits are expressed, the neuronal erg current in these cells could be carried by erg channels mainly composed of erg1a and erg3 subunits.

If we assume that the four different erg channel subunits detected in serotonergic neurones have the same chance to take part in the formation of a functional

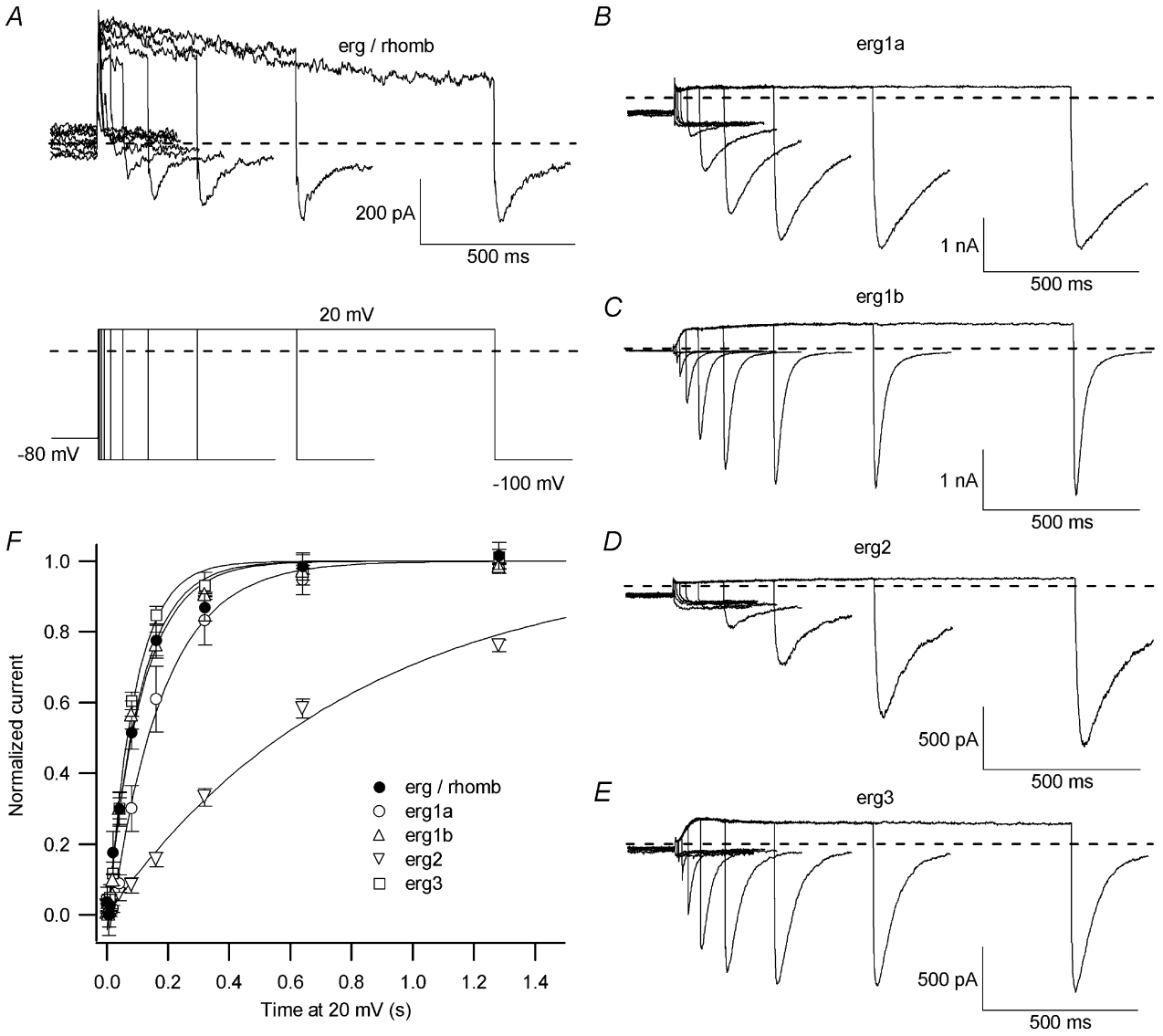

Figure 10. Time course of erg current activation

The time dependence of erg current activation from embryonic rhombencephalon neurones (*A*, E-4031-sensitive current) compared with erg1a (*B*), erg1b (*C*), erg2 (*D*) and erg3 (*E*) currents expressed in CHO cells. *A*, part of the outward currents were probably due to rundown artefacts of an outwardly rectifying K^+ current. The envelope-of-tail protocol (see pulse diagram) consisted of the following pulse sequence: from a holding potential of −80 mV a pulse to 20 mV of increasing duration was followed by a subsequent voltage step to −100 mV eliciting an inward tail current. The mean normalized peak tail current amplitudes of native erg current (●, $n = 7$) as well as of erg1a (○; $n = 5$), erg1b (Δ; $n = 11$), erg2 (∇; $n = 9$) and erg3 (□; $n = 4$) currents were plotted against the duration of the pulse to 20 mV (*F*). The time constants of activation (τ) were determined by fitting the curves with a single exponential function.

erg channel, then numerous channel compositions could be possible. However, since the biophysical properties of the majority of the rhombencephalic erg currents were astonishingly homogeneous, one could assume that there may exist intracellular mechanisms leading to the formation of predominantly one type of heteromeric erg channel with a defined subunit composition comparable to the defined subunit composition of the nicotinic acetylcholine receptor (reviewed in Wanamaker *et al.* 2003). However, the sorting mechanism could be different in neurones and for example rat lactotropes, since in both cell types the same erg subunits are coexpressed, but the biophysical properties of the erg currents are different (Schäfer *et al.* 1999; this work). Direct experimental evidence of the subunit composition of the neuronal erg channels by coimmunoprecipitation would require antibodies against the involved erg subunits, but only antibodies against erg1 channels are as yet available. In principle, differences between the properties of neuronal and heterologously expressed currents could also be due to different degrees of phosphorylation of the channel protein (Wei *et al.* 2002; Cayabyab & Schlichter, 2002), activation of different intracellular signal cascades by neurotransmitters and hormones (Bian *et al.* 2001; Schledermann *et al.* 2001; Hirdes *et al.* 2004), the association of erg channels with β subunits or the expression of as yet unknown erg splice variants (see Bauer & Schwarz, 2001).

Comparison of the erg current in raphe neurones with other native erg currents

Erg currents in cells of the somatomammotrope cell line GH_3/B_6 and those of erg1a currents after heterologous expression in CHO cells recorded under the same experimental conditions (isotonic KCl, nanomolar concentration of external Ca^{2+} concentration) are very similar, e.g. the time course of deactivation is almost identical as well as the voltage dependence of the availability curves (Bauer *et al.* 1998). This is in accordance with the expression of mRNA for erg1a and erg2, and the lack of erg3 (Wulfsen *et al.* 2000) and erg1b (I. Wulfsen, unpublished observations) which both exhibit faster gating kinetics. If compared to the erg current in lactotrope cells, the erg current in raphe neurones can be characterized as 'fast'. Fast deactivation kinetics have also be observed, for example, in native erg currents of portal vein myocytes (Ohya *et al.* 2002*b*), neuroblastoma cells (Arcangeli *et al.* 1995), cerebellar Purkinje cells and cardiac myocytes.

So far, one detailed report about another neuronal erg current has been published and this is in mouse cerebellar Purkinje neurones (Sacco *et al.* 2003). In that study similar recording conditions were used to those in the present experiments allowing a direct comparison. In both preparations the time constants describing deactivation proceeded fast, with $\tau_{deact} = 200$ and 80 ms at -70 and -90 mV, respectively, in Purkinje neurones and $\tau_{deact} = 230$ and 83 ms, respectively, in serotonergic neurones. This is in contrast to $\tau_{deact} = 436$ ms at -90 mV in heterologously expressed erg1a currents (see Fig. 7). At -70 mV, in erg1a currents deactivation proceeds so slowly that a time constant was not determined (see Fig. 6*B*). Since in Purkinje cells, erg1 and erg3 channel subunits (Saganich *et al.* 2001) or even all three erg subunits (Papa *et al.* 2003) are expressed, as in rhombencephalon neurones, it is possible that heteromeric erg channels with similar subunit composition and properties are formed in Purkinje cells and raphe neurones.

Also the cardiac rapidly activating K^+ current (I_{Kr}) known to be mediated by erg1 channels (Sanguinetti *et al.* 1995) deactivates considerably faster than the heterologously expressed erg1a (HERG) current. One explanation for this discrepancy is the coexpression of HERG1b in the heart (Lees-Miller *et al.* 1997; London *et al.* 1997). Using heterologous expression, it has been demonstrated that erg1a and erg1b tend to coassemble to heteromeric erg1 channels with intermediate deactivation kinetics (London *et al.* 1997). Recently, coimmunoprecipitation experiments confirmed that native I_{Kr} channels indeed involve heteromultimers of HERG1a and HERG1b (Jones *et al.* 2004). Compared to the abundant expression in heart, erg1b is only weakly expressed in brain (Lees-Miller *et al.* 1997; Ohya *et al.* 2002*b*), and also no expression of erg1b in brain was reported by London *et al.* (1997) and Pond *et al.* (2000). Our results using Western blots of adult whole rat brain confirm the weaker expression of erg1b compared to erg1a. In contrast, in embryonic rhombencephalon, we found a comparable expression of erg1a and erg1b protein which is paralleled by the single-cell RT-PCR detecting erg1b in about 40% of the investigated rhombencephalon cells.

The slow component of erg current

About 20% of the rhombencephalon neurones exhibit a slowly deactivating erg current component associated with a midpoint potential of the availability curve located at a very negative membrane potential of about -110 mV. An almost identical slowly deactivating erg current component was described in native lactotropes (Corrette *et al.* 1996; Schäfer *et al.* 1999) and in the lactotrope MMQ cell line (Lecchi *et al.* 2002). In contrast to rhombencephalic neurones, the slow erg current component is present in almost all native lactotropes and MMQ cells. In lactotropes, the contribution of the slowly deactivating current component to the total erg current amplitude varies from cell to cell (Schäfer *et al.* 1999). The fast and the slowly deactivating erg current components in MMQ cells have been shown to modulate frequency adaptation as well as prolactin secretion on a fast (within

about 1 s) and a slow time scale (within about 1 min) (Lecchi *et al.* 2002). Obviously, the slowly deactivating erg current is not a unique phenomenon of lactotropes.

Possible function of the neuronal erg current

Possible functions for erg currents in the brain have been discussed for hippocampal astrocytes (Emmi *et al.* 2000), cerebellar Purkinje neurones (Sacco *et al.* 2003) and dopaminergic neurones (Nedergaard, 2004). In astrocytes the erg1 current has been assumed to play a role for K^+ homeostasis. In Purkinje neurones, blocking the erg current led to a small depolarization and a tendency towards increased action potential firing. In substantia nigra pars compacta neurones an erg current has been assumed to play a role in the slow component of the afterhyperpolarization (Nedergaard, 2004). As yet our preliminary current-clamp results have not demonstrated a distinct functional role for the rhombencephalic erg current. In an intact neuronal network one would expect an increase in the cellular excitability when the erg current is reduced, e.g. by hormones or neurotransmitters (Bauer *et al.* 1999; Bian *et al.* 2001; Schledermann *et al.* 2001; Hirdes *et al.* 2004). On the other hand, the faster activation kinetics of the neuronal erg current described in the present paper could well explain the fast erg-mediated frequency adaptation observed in cerebellar Purkinje neurones (Sacco *et al.* 2003). Finally, serotonin release could be influenced by modulation of the erg current at axon terminals. Studies in combination with erg knockout mutants or knockdown with siRNA are planned to reveal a role of the different erg subunits in the normal and abnormal activity of the brain.

References

Arcangeli A, Becchetti A, Mannini A, Mugnai G, De Filippi P, Tarone G *et al.* (1993). Integrin-mediated neurite outgrowth in neuroblastoma cells depends on the activation of potassium channels. *J Cell Biol* **122**, 1131–1143.

Arcangeli A, Bianchi L, Becchetti A, Faravelli L, Coronnello M, Mini E *et al.* (1995). A novel inward-rectifying K^+ current with a cell-cycle dependence governs the resting potential of mammalian neuroblastoma cells. *J Physiol* **489**, 455–471.

Barros F, Delgado LM, del Camino D & de la Peña P (1992). Characteristics and modulation by thyrotropin-releasing hormone of an inwardly rectifying K^+ current in patch-perforated GH_3 anterior pituitary cells. *Pflugers Arch* **422**, 31–39.

Bauer CK, Engeland B, Wulfsen I, Ludwig J, Pongs O & Schwarz JR (1998). RERG is a molecular correlate of the inward-rectifying K current in clonal rat pituitary cells. *Receptors Channels* **6**, 19–29.

Bauer CK, Meyerhof W & Schwarz JR (1990). An inward-rectifying K^+ current in clonal rat pituitary cells and its modulation by thyrotrophin-releasing hormone. *J Physiol* **429**, 169–189.

Bauer CK, Schäfer R, Schiemann D, Reid G, Hanganu I & Schwarz JR (1999). A functional role of the erg-like inward-rectifying K^+ current in prolactin secretion from rat lactotrophs. *Mol Cell Endocrinol* **148**, 37–45.

Bauer CK & Schwarz JR (2001). Physiology of EAG K^+ channels. *J Membr Biol* **182**, 1–15.

Bayliss DA, Li YW & Talley EM (1997). Effects of serotonin on caudal raphe neurons: activation of an inwardly rectifying potassium conductance. *J Neurophysiol* **77**, 1349–1361.

Bian J, Cui J & McDonald TV (2001). HERG K^+ channel activity is regulated by changes in phosphatidyl inositol 4,5-bisphosphate. *Circ Res* **89**, 1168–1176.

Cayabyab FS & Schlichter LC (2002). Regulation of an ERG K^+ current by Src tyrosine kinase. *J Biol Chem* **277**, 13673–13681.

Chiesa N, Rosati B, Arcangeli A, Olivotto M & Wanke E (1997). A novel role for HERG K^+ channels: spike-frequency adaptation. *J Physiol* **501**, 313–318.

Corrette BJ, Bauer CK & Schwarz JR (1996). An inactivating inward-rectifying K current present in prolactin cells from the pituitary of lactating rats. *J Membr Biol* **150**, 185–195.

Crociani O, Cherubini A, Piccini E, Polvani S, Costa L. Fontana L *et al.* (2000). Erg gene(s) expression during development of the nervous and muscular system of quail embryos. *Mech Dev* **95**, 239–243.

Curran ME, Splawski I, Timothy KW, Vincent GM, Green ED & Keating MT (1995). A molecular basis for cardiac arrhythmia: HERG mutations cause long QT syndrome. *Cell* **80**, 795–803.

Emmi A, Wenzel HJ, Schwartzkroin PA, Taglialatela M, Castaldo P, Bianchi L *et al.* (2000). Do glia have heart? Expression and functional role for ether-a-go-go currents in hippocampal astrocytes. *J Neurosci* **20**, 3915–3925.

Eng LF, Ghirnikar RS & Lee YL (2000). Glial fibrillary acidic protein: GFAP-thirty-one years (1969–2000). *Neurochem Res* **25**, 1439–1451.

Gessner G & Heinemann SH (2003). Inhibition of hEAG1 and hERG1 potassium channels by clofilium and its tertiary analogue LY97241. *Br J Pharmacol* **138**, 161–171.

Grahame-Smith DG (1964). Tryptophan hydroxylation in brain. *Biochem Biophys Res Commun* **16**, 586–592.

Hirdes W, Horowitz LF & Hille B (2004). Muscarinic modulation of erg potassium current. *J Physiol* **559**, 67–84.

Jones EM, Roti Roti EC, Wang J, Delfosse SA & Robertson GA (2004). Cardiac I_{Kr} channels minimally comprise hERG1a and 1b subunits. *J Biol Chem* **279**, 44690–44694.

König N, Han V, Lieth E & Lauder J (1987). Effects of coculture on the morphology of identified raphe and substantia nigra neurons from the embryonic rat brain. *J Neurosci Res* **17**, 349–360.

Lecchi M, Redaelli E, Rosati B, Gurrola G, Florio T, Crociani O *et al.* (2002). Isolation of a long-lasting eag-related gene-type K^+ current in MMQ lactotrophs and its accommodating role during slow firing and prolactin release. *J Neurosci* **22**, 3414–3425.

Lees-Miller JP, Kondo C, Wang L & Duff HJ (1997). Electrophysiological characterization of an alternatively processed ERG K^+ channel in mouse and human hearts. *Circ Res* **81**, 719–726.

London B, Trudeau MC, Newton KP, Beyer AK, Copeland NG, Gilbert DJ *et al.* (1997). Two isoforms of the mouse ether-a-go-go-related gene coassemble to form channels with properties similar to the rapidly activating component of the cardiac delayed rectifier K^+ current. *Circ Res* **81**, 870–878.

Monyer H & Jonas P (1995). Polymerase chain reaction analysis of ion channel expression in single neurons of brain slices. In *Single-Channel Recording*, 2nd edn, ed. Sakmann B & Neher E, pp. 357–373. Plenum Press, New York.

Nedergaard S (2004). A Ca^{2+}-independent slow afterhyperpolarization in substantia nigra compacta neurons. *Neuroscience* **125**, 841–852.

Ohya S, Asakura K, Muraki K, Watanabe M & Imaizumi Y (2002*a*). Molecular and functional characterization of ERG, KCNQ, and KCNE subtypes in rat stomach muscle. *Am J Physiol Gastrointest Liver Physiol* **282**, G277–G287.

Ohya S, Horowitz B & Greenwood IA (2002*b*). Functional and molecular identification of ERG channels in murine portal vein myocytes. *Am J Physiol Cell Physiol* **283**, C866–C877.

Papa M, Boscia F, Canitano A, Castaldo P, Sellitti S, Annunziato L *et al.* (2003). Expression pattern of the ether-a-gogo-related (ERG) K^+ channel-encoding genes ERG1, ERG2, and ERG3 in the adult rat central nervous system. *J Comp Neurol* **466**, 119–135.

Patel PD, Pontrello C & Burke S (2004). Robust and tissue-specific expression of TPH2 versus TPH1 in rat raphe and pineal gland. *Biol Psychiatry* **55**, 428–433.

Polvani S, Masia A, Pillozzi S, Gragnani L, Crociani O, Olivotto M *et al.* (2003). Developmentally regulated expression of the mouse homologues of the potassium channel encoding genes m-erg1, m-erg2 and m-erg3. *Gene Expr Patterns* **3**, 767–776.

Pond AL, Scheve BK, Benedict AT, Petrecca K, Van Wagoner DR, Shrier A *et al.* (2000). Expression of distinct ERG proteins in rat, mouse, and human heart. Relation to functional I_{Kr} channels. *J Biol Chem* **275**, 5997–6006.

Sacco T, Bruno A, Wanke E & Tempia F (2003). Functional roles of an ERG current isolated in cerebellar Purkinje neurons. *J Neurophysiol* **90**, 1817–1828.

Saganich MJ, Machado E & Rudy B (2001). Differential expression of genes encoding subthreshold-operating voltage-gated K^+ channels in brain. *J Neurosci* **21**, 4609–4624.

Sanguinetti MC, Jiang C, Curran ME & Keating MT (1995). A mechanistic link between an inherited and an acquired cardiac arrhythmia: HERG encodes the I_{Kr} potassium channel. *Cell* **81**, 299–307.

Schäfer R, Wulfsen I, Behrens S, Weinsberg F, Bauer CK & Schwarz JR (1999). The erg-like potassium current in rat lactotrophs. *J Physiol* **518**, 401–416.

Schledermann W, Wulfsen I, Schwarz JR & Bauer CK (2001). Modulation of rat erg1, erg2, erg3 and HERG K^+ currents by thyrotropin-releasing hormone in anterior pituitary cells via the native signal cascade. *J Physiol* **532**, 143–163.

Schönherr R, Rosati B, Hehl S, Rao VG, Arcangeli A, Olivotto M *et al.* (1999). Functional role of the slow activation property of ERG K^+ channels. *Eur J Neurosci* **11**, 753–760.

Schwarz JR, Schweizer M, Schuricht K, Schledermann W & Glassmeier G (2003). Erg potassium channels in rat nucleus raphe neurons. *Program No. 53.7 2003 Abstract Viewer/Itinerary Planner*. Society for Neuroscience, Washington, DC, USA.

Shi W, Wymore RS, Wang HS, Pan Z, Cohen IS, McKinnon D *et al.* (1997). Identification of two nervous system-specific members of the erg potassium channel gene family. *J Neurosci* **17**, 9423–9432.

Shibasaki T (1987). Conductance and kinetics of delayed rectifier potassium channels in nodal cells of the rabbit heart. *J Physiol* **387**, 227–250.

Spector PS, Curran ME, Keating MT & Sanguinetti MC (1996). Class III antiarrhythmic drugs block HERG, a human cardiac delayed rectifier K^+ channel. Open-channel block by methanesulfonanilides. *Circ Res* **78**, 499–503.

Törk I (1985). Raphe nuclei and serotonin containing systems. In *The Rat Nervous System*, ed.Paxinos G, pp. 43–78. Academic Press, Sydney, Australia.

Trudeau MC, Warmke JW, Ganetzky B & Robertson GA (1995). HERG, a human inward rectifier in the voltage-gated potassium channel family. *Science* **269**, 92–95.

Walther DJ & Bader M (2003). A unique central tryptophan hydroxylase isoform. *Biochem Pharmacol* **66**, 1673–1680.

Wanamaker CP, Christianson JC & Green WN (2003). Regulation of nicotinic acetylcholine receptor assembly. *Ann N Y Acad Sci* **998**, 66–80.

Wang S, Liu S, Morales MJ, Strauss HC & Rasmusson RL (1997). A quantitative analysis of the activation and inactivation kinetics of HERG expressed in *Xenopus* oocytes. *J Physiol* **502**, 45–60.

Warmke JW & Ganetzky B (1994). A family of potassium channel genes related to eag in *Drosophila* and mammals. *Proc Natl Acad Sci U S A* **91**, 3438–3442.

Wei Z, Thomas D, Karle CA, Kathofer S, Schenkel J, Kreye VA *et al.* (2002). Protein kinase A-mediated phosphorylation of HERG potassium channels in a human cell line. *Chin Med J (Engl)* **115**, 668–676.

Weinsberg F, Bauer CK & Schwarz JR (1997). The class III antiarrhythmic agent E-4031 selectively blocks the inactivating inward-rectifying potassium current in rat anterior pituitary tumor cells (GH_3/B_6 cells). *Pflugers Arch* **434**, 1–10.

Wimmers S, Bauer CK & Schwarz JR (2002). Biophysical properties of heteromultimeric erg K^+ channels. *Pflugers Arch* **445**, 423–430.

Wimmers S, Wulfsen I, Bauer CK & Schwarz JR (2001). Erg1, erg2 and erg3 K channel subunits are able to form heteromultimers. *Pflugers Arch* **441**, 450–455.

Wulfsen I, Hauber H-P, Schiemann D, Bauer CK & Schwarz JR (2000). Expression of mRNA for voltage-dependent and inward-rectifying K channels in GH_3/B_6 cells and rat pituitary. *J Neuroendocr* **12**, 263–272.

Acknowledgements

We thank Saskia Siegel, Dorrit Schiemann, and Waltraud Krüger for technical assistance. This work was supported by the Deutsche Forschungsgemeinschaft (SFB 444 (A3) and GK 255.